

EARLY SHAPING OF ASYMMETRICAL PLANETARY NEBULAE

NOAM SOKER

Department of Astronomy, University of Virginia

Received 1988 August 8; accepted 1988 October 24

ABSTRACT

We suggest that the shape of a young asymmetrical planetary nebulae may be influenced by a close binary-star located at its center. This binary is a relic of the common envelope phase, presumably through which the asymmetrical planetary nebula evolved. We assume that for a short period of time, shortly after the cessation of the slow wind and long before the fast wind becomes effective, the binary ejects a small amount of mass, mainly in the equatorial plane. In this work we do not discuss the exact mechanism for the ejection of this pulse of mass. By using two-dimensional hydrodynamics we find that at late times the high-density region has a "horseshoe" shape, as viewed in the symmetry plane. There is an instability in the maximum density region, which shows up as a high-density knot. The exact scale of the knot is determined by the numerics. We comment about the applications of our results to observations.

Subject headings: hydrodynamics — nebulae: planetary — stars: binaries

I. INTRODUCTION

The model for shaping planetary nebulae (PNe) via the interaction between a fast wind from the hot central star, and a slow wind resulting from the ejection of the progenitor red giant envelope, has had considerable success in explaining various features in the morphology of PNe (see, e.g., Kwok 1982; Volk and Kwok 1985). As many of the PNe have aspherical morphologies, a number of works have tried to explain them in the framework of the interacting winds model (Kahn and West 1985; Balick 1987; Balick, Preston, and Icke 1987). Recently, Soker and Livio (1989, hereafter referred to as SL), using a two-dimensional hydrodynamic numerical code, have shown that interacting winds are capable of producing morphologies similar to the ones observed in asymmetrical PNe. They have also discussed mechanisms that can produce the enhanced density in the equatorial plane, required for the formation of asymmetric PNe according to the model. Based on the results of Livio and Soker (1988) they claim that the most natural mechanism is the common envelope one.

In most of the above calculations, it has been assumed that both the slow and the fast winds are each characterized by a constant mass-loss rate and velocity. However, this is not exactly the case. The fast wind from the hot central star evolves continuously: the mass-loss rate decreases with time and the velocity increases (Volk and Kwok 1985). In addition, towards the end of the red-giant phase, the mass-loss rate in the slow wind increases (Harpaz and Kovetz 1981) and so does the velocity. The fast wind starts ~ 1000 yr after the cessation of the slow wind (Volk and Kwok 1985). In the light of these points, it seems the interaction process is much more complicated than was assumed in earlier models, especially during the transition time between the winds. However, as there are many uncertainties in the exact evolution of the winds, and in order to solve the problem in a reasonable manner, we will adopt the simple assumptions mentioned above.

In this work we examine the possibility that for a short period of time, immediately after the cessation of the slow wind, the close binary that is left after the common envelope phase ejects a small amount of mass close to the equatorial plane. (We therefore follow SL in assuming that a binary-star system is the common cause of asymmetrical PNe.) This

ejected mass pulse can shape the PNe before the fast wind becomes effective.

The method of calculation and the model are presented in § II. The results of the numerical calculation are presented in § III and in § IV we discuss them.

II. METHOD OF CALCULATION AND THE MODEL

We presently use the same numerical hydrodynamic code that has been used by SL in their calculations of interacting winds in PNe. It is a two-dimensional time-dependent particle-in-cell (PIC) hydrodynamical scheme. The PIC scheme contains an Eulerian grid made up of cells and a Lagrangian grid made up of particles. The physical variables are calculated at each time step in each cell by averaging over the physical variables of all particles residing in that cell. The particles are moved in each time step, and as each particle has mass, energy and velocity, the motion of the particles takes care of the advection terms in the hydrodynamic equations. The physical variables of each particle are changed at each time step due to interaction with all the particles located at the same cell. This interaction causes numerical viscosity and heat conduction. The strength of this interaction is determined by a parameter α , which was set, as in SL, to be 1 in the primary cells grid and 0.3 in the secondary cells grid. The role of the secondary cells grid is to form an interaction between the cells of the primary grid. For more detailed description of this scheme see Livio *et al.* (1986) and Soker *et al.* (1987). Because of the fluctuations in number of particles residing at neighboring cells, previous work with this numerical scheme indicates that we need more than about six particles per cell on average. Even with many more particles per cell, the fluctuations between neighboring cells can be quite high. We will return to this point when we discuss the instability in the high-density region.

In choosing the parameters for the calculation to be described below, we took into account numerical constraints, including resolution, computer time, and memory. Due to the symmetry of the problem, our two-dimensional grid contains only one-quarter of the symmetry plane, which was resolved by a Cartesian grid of 200×100 cells, each having a size of 5×10^{14} cm. For the mass-loss rate and velocity of the slow wind we took $\dot{M}_1 = 10^{-5} M_{\odot} \text{ yr}^{-1}$, $V_1 = 10 \text{ km s}^{-1}$, respec-

tively. The Mach number of the slow wind was 15 and the density profile according to

$$\rho \propto (1 + a \cos^4 \theta), \quad (1)$$

where θ is the angle from the equatorial plane. As the velocity of the wind is constant, its density as a function of radial distance falls like r^{-2} . Based on the results of SL, we took $a = 5$. From the differences they found in their calculations of interacting winds with $a = 15$, we conclude that we would have found no big differences in our calculation had we taken any a such that $1 \lesssim a \lesssim 20$.

The ejected mass in the pulse was $3 \times 10^{-4} M_{\odot}$. We chose this somewhat arbitrary number based on the results of Harpaz and Kovetz (1981), who found that when the mass of the red-giant envelope becomes $\sim 10^{-3} M_{\odot}$ the envelope's radius contracts substantially. For the velocity of the ejected mass we took a typical escape velocity from the binary-stars system, $v_{ej} = 200 \text{ km s}^{-1}$ in a radial direction,

$$v_{ej} \simeq \left(\frac{2GM}{s} \right)^{1/2} = 200 \text{ km s}^{-1} \left(\frac{M}{M_{\odot}} \right)^{1/2} \left(\frac{s}{10 R_{\odot}} \right)^{-1/2}, \quad (2)$$

where M is the binary mass and s is the size of the binary-stars system. Its Mach number was taken to be 60. The density profile of the ejected mass was taken somewhat arbitrarily to be $\rho \propto (0.04 - \sin^2 \theta)$ for $|\sin \theta| < 0.2$ and zero elsewhere. The pulse was started 600 yr after the cessation of the slow wind and its duration was 50 yr. As the ejected mass does not cover the full sphere, we do not expect that a hot, low-density bubble will be formed in the center (unlike the case in the interacting winds model). This will cause a drop in the pressure, due to leakage of hot gas (see discussion by SL), which behaves like an effective cooling of the gas. In order to simulate this effective cooling we took the adiabatic index to be $\gamma = 1.1$. The removal of particles with negative radial velocity (see LS) also contributes to the effective cooling, although it is less important than

in SL. The initial number of particles representing the slow wind in the grid was 135×10^3 and the ejected mass was represented by 21×10^3 particles.

III. NUMERICAL RESULTS

We present our results as density contours and velocity maps at four different times in Figures 1–4. In these figures the Y axis is taken along the symmetry axis and the X axis is taken to be in the equatorial plane. Before we discuss the results, a few numerical features should be noted: (i) The numerical code has problems close to the Y axis, and hence the results in this region should be taken with caution. Fortunately, this has no effect on the results in the regions that interest us. (ii) Due to the finite number of particles in each cell, the results in very low density regions should also be taken cautiously. This, however, does not influence the main flow. (iii) The high-density peaks are the results of an instability. Nagasawa, Nakamura, and Miyama (1988), using three-dimensional hydrodynamics, obtained the same type of density morphology caused by an instability inside the shell of a supernova explosion. They interpreted this as a Rayleigh-Taylor instability. Such an instability causes the initial density fluctuations, due to finite number of particles per cell, to increase substantially. The instability occurs only in a thin shell, at the maximum density region. Although this feature is probably physical, the exact density contrast of the knots and their sizes depend on the numerical parameters. Due to our high numerical viscosity and finite resolution, one should be cautious in drawing conclusions about instability from our calculation. In any case, as the instability knots are very small, only $\sim 10^{15}$ cm in size, and their density is less than twice the maximum density in the ‘‘horseshoe,’’ it is likely that they will not be resolved by observations.

At early times (Fig. 1), the high-density region takes the shape of a ring. At later times the high-density region turns

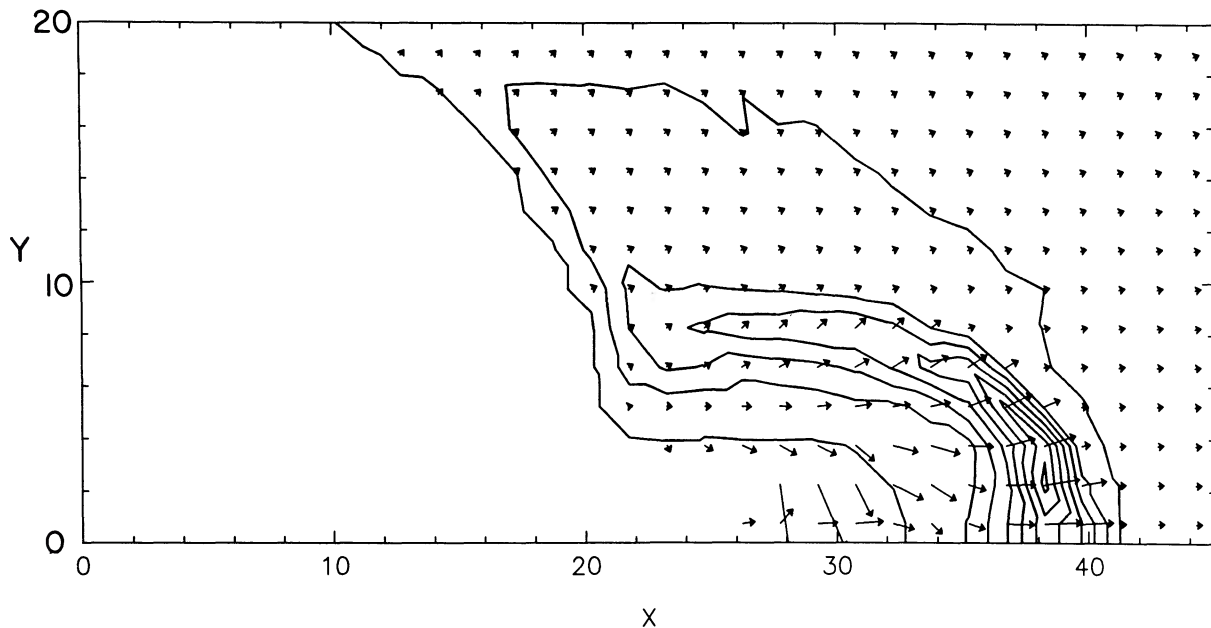


FIG. 1.—Density contours and velocity field map at time $t = 90$ yr from the time the pulse reaches the slow wind. The units on the axes are 10^{15} cm. Each unit length (as measured on the axes) of the arrows corresponds to a velocity of 40 km s^{-1} , and the density levels, in units of $10^{-21} \text{ g cm}^{-3}$, are 5, 50, 100, 150, 200, 250, 300, 350.

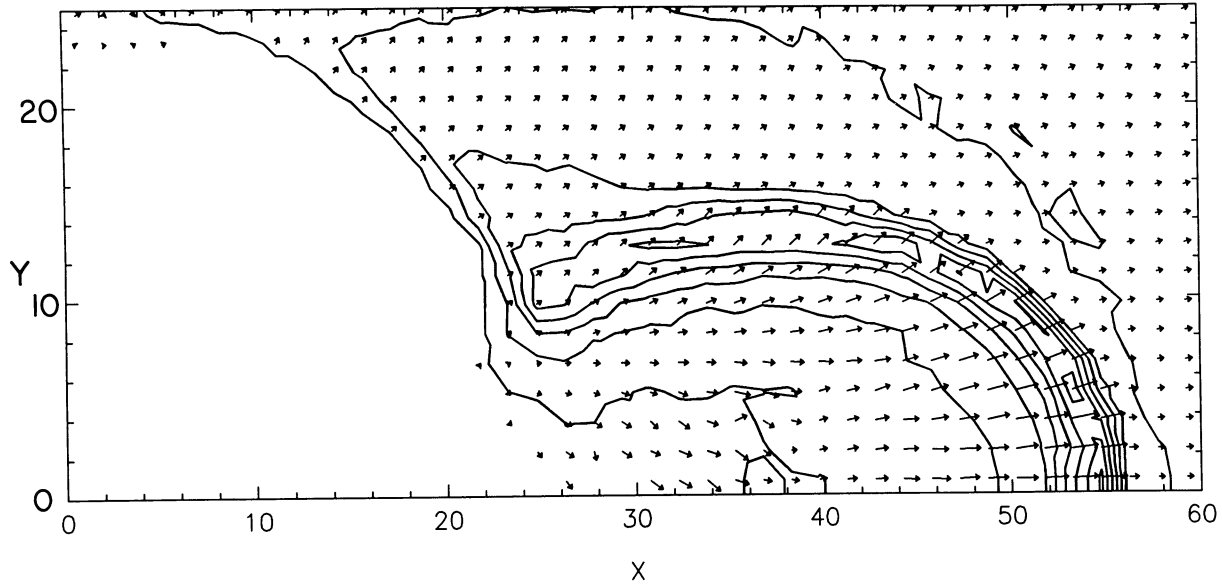


FIG. 2.—Like Fig. 1 but at time $t = 190$ yr. Each unit length (as measured on the axes) of the arrows corresponds to a velocity of 28 km s^{-1} , and the density levels, in units of $10^{-21} \text{ g cm}^{-3}$, are 5, 25, 50, 75, 100, 125, 150, 175.

into a “horseshoe” shape, as viewed in the symmetry plane (Figs. 2, 3, and 4). At much later time (Fig. 4), the maximum density region is not continuous, but rather is composed of two main regions. The first one is in the outer part (the part further away from the center) of the “horseshoe” but detached from the equatorial plane; the second region is in the inner part of the “horseshoe.” In a more realistic situation, where the pulse of mass ejection does not end sharply, we expect the inner part of the “horseshoe” to be pushed away by continuous mass ejection, and so to be less prominent than in our results. In Figure 4 the maximum density region is approximately circular (torus in three dimensions). This resembles the shape of a point explosion as viewed in two dimensions, similar to a

supernova, for example (Nagasawa, Nakamura, and Miyama 1988). This is because the pulse of ejected mass is short and interacts with the slow wind in a small volume, and so the dissipation creates a high-pressure region. Here also, we expect that in a more realistic situation this effect will be less prominent than we find in our calculation. As we expect, the flow velocity decreases with time. The maximum velocities in the equatorial plane are 60, 40, 32, and 25 km s^{-1} in Figures 1, 2, 3, and 4, respectively.

IV. DISCUSSION

We have suggested here that the morphologies of very young asymmetrical PNe can be influenced by a close binary

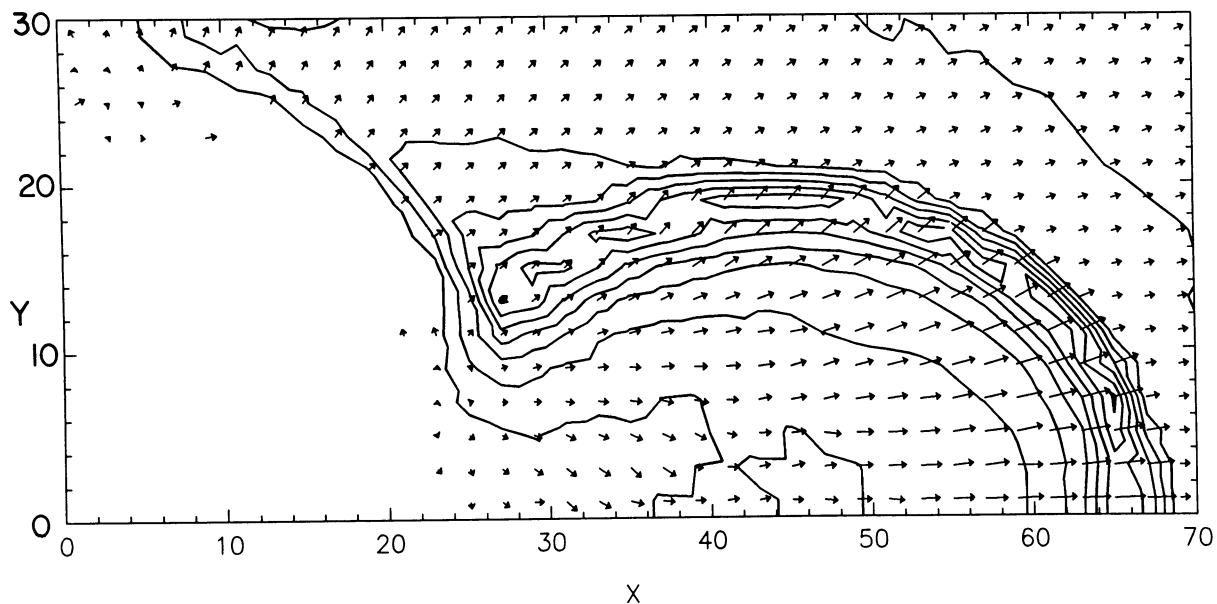


FIG. 3.—Like Fig. 1 but at time $t = 280$ yr. Each unit length (as measured on the axes) of the arrows corresponds to a velocity of 17 km s^{-1} , and the density levels, in units of $10^{-21} \text{ g cm}^{-3}$, are 5, 15, 30, 45, 60, 75, 90, 105.

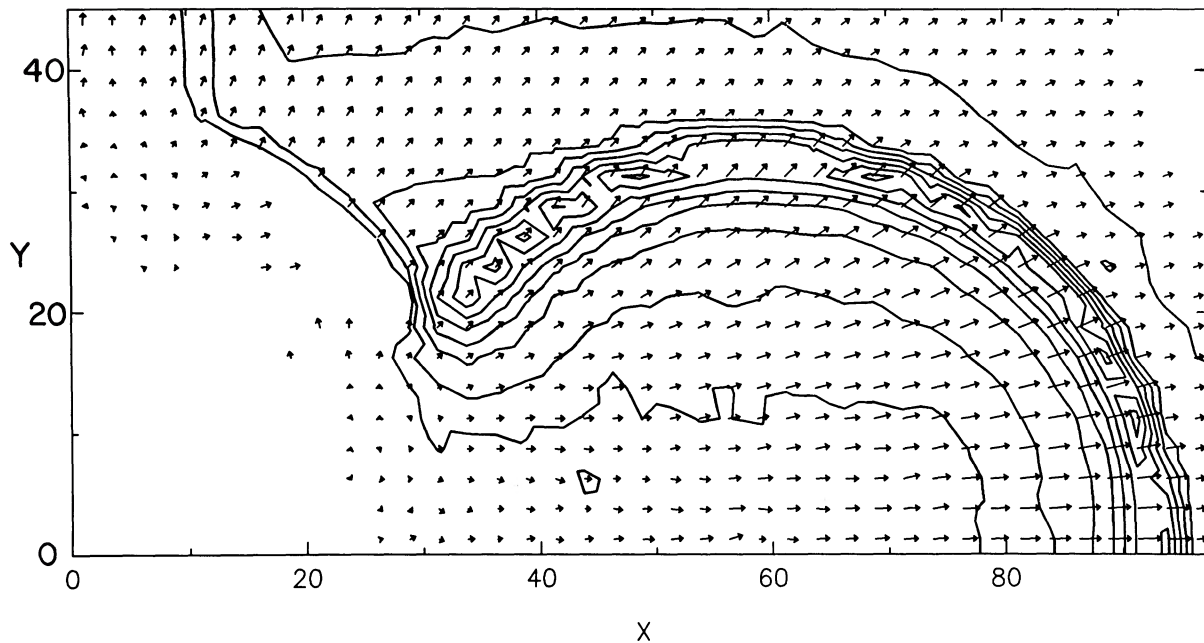


FIG. 4.—Like Fig. 1 but at time $t = 570$ yr. Each unit length (as measured on the axes) of the arrows corresponds to a velocity of 12 km s^{-1} , and the density levels, in units of $10^{-21} \text{ g cm}^{-3}$, are 4, 8, 16, 24, 32, 40, 48, 56.

located at the center of the PNe. In this work we have calculated the effect of mass ejected for a short period of time close to the equatorial plane by the binary. Although we did not discuss the mechanism for ejecting this pulse of mass, it may be that the mass leaves the binary through the second Lagrangian point, as in the mechanism suggested by Livio, Salzman, and Shaviv (1979). Another possibility, although rather extreme, is that towards the end of the red giant phase the secondary star collides with the core of the red giant. In this case, mass can be blown away in the equatorial plane in a way similar to that obtained in the collision of a $0.2 M_{\odot}$ main-sequence star with a white dwarf in the calculations of Soker *et al.* (1987). This might be the case for a low-mass secondary star. As was discussed by Livio and Soker (1984), a common envelope phase can end (in principle) in three ways. For a sufficiently massive secondary, a close binary will be left in the end. For a low-mass secondary, two things may happen: the secondary may collide with the core, or a very low mass secondary (brown dwarf) may be evaporated inside the red giant envelope while accreting mass. The destiny of the secondary also depends on the structure of the red giant, since it will have more chances to survive in a more evolved giant. The last two scenarios suggest that we may find a very asymmetrical PN which does not contain a close binary in the center, even when the asymmetry was caused by the common envelope mechanism. Collision of the two stars inside a common envelope, which was a progenitor of a PN, was suggested recently by Mendeze *et al.* (1988), as an explanation for two PNe (125-47 1 and 212+23 1). Since these PNe have large radii (~ 0.25 pc, Mendez *et al.*, 1988), and are therefore probably old PNe, we cannot apply our model to them.

We want to emphasize again the assumptions concerning the evolution of the winds. As we point out in the Introduction, the real situation, especially in the transition period between the winds, is much more complicated than what we assume here. However, in order to be able to solve the problem, a simple form for the slow and fast winds is usually assumed. We

have done the same thing here by assuming a simple form for the pulse of ejected mass. In addition to a nonconstant mass-loss rate and a nonconstant velocity for the slow wind, we expect that the transition from the slow wind to the ejected mass pulse will be much smoother than what we have assumed here. We feel, however, that our calculation gives the gross features of what might happen, under certain circumstances, in PNe going through a common envelope phase.

In order to reproduce a picture of a PN, we need to do a full calculation of the radiative transfer problem, and to include projection effects, which are beyond the scope of this work. We point here only to the brightest regions of a few PNe (e.g., MZ-3, Perek and Kohoutek 1967) and proto-PNe that have a shape similar to the one we obtain at late times in our numerical calculation, if viewed edge-on and if ionizing radiation starts before the fast wind. (However, this is probably not the case in most objects.) In the case of MZ-3 (among others), a bipolar outflow is probably the reason for the observed morphology (e.g. Meaburn, Walsh, and Clayton 1985). If the mechanism we suggest here is responsible for the morphology of part of these PNe, then they may have a binary at their center (if the two stars did not collide as discussed above). Based on the mechanism discussed in Livio, Salzman, and Shaviv (1979), Livio (1982) already suggested that PNe having such a morphology should be searched for a binary located at their center. Here we only raise the possibility that this kind of morphology in very young PNe may be a consequence of the mechanism we proposed above, if viewed edge-on.

More relevant cases can be proto-PNe, such as CRL 2688. The model for CRL 2688 is a bipolar outflow, caused by a fast wind from the central star shaped by a molecular ring (see Kawabe *et al.* [1987] and references therein). The distance of the outer lobes from the center in CRL 2688 is $\sim 2.5 \times 10^{17}$ cm. In this object it seems that the fast wind from the central star starts before the ionizing radiation (Beckwith, Beck, and Gatley 1984). If this is typical in proto-PNe, then we expect to see the horseshoe shape only in lines resulting from collisional

excitation or in reflection light from the central star and then only at very early times of order a few hundreds years. This raises another possible role for the mass ejected in the equatorial plane. It may be that the ejected mass, together with the mass it swept from the slow wind, forms the molecular ring responsible for shaping the fast wind to a bipolar outflow. In the model for CRL 2688 of Kawabe *et al.* (1987), the radius of this ring is of the order of few times 10^{16} cm, and they claim that the age of the flow is $\sim 10^3$ yr. Our calculation gives this order of distances for the ring at few hundreds years, especially if we take a lower velocity for the ejected pulse of mass. Since the velocity of this ring is very low at late times, the shock excitation is not efficient, and this ring will not be observed in optical light. At late times of a few thousands years, after the fast wind becomes effective, the ring cause by the ejected mass will disappear and the system will have the typical morphology of the interacting winds model.

To summarize, the shaping of very young PNe in the tran-

sition period between winds is a complicated problem, as the wind properties are not constant. The shaping of a very young PN having a binary in the center may be much more complicated, since the binary can play a role. In this work, we have shown how mass ejected close to the equatorial plane after the cessation of the slow wind, presumably by the binary, can form a horseshoe shape in young PNe. This ring can also be responsible for shaping a bipolar outflow in proto-PNe. These types of morphologies in young PNe may indicate the presence of a binary at the centers of the PNe, or a recent collision of the two stars in the center.

I thank Peter Becker, Mario Livio, Eric Myra, and Oded Regev for carefully reading the manuscript of this paper. I also thank the Pittsburgh Supercomputer Center for providing computing time on a Cray supercomputer. This work has been supported in part by the NASA Astrophysical Theory Center grant NAGW-764.

REFERENCES

- Balick, B. 1987, *A.J.*, **94**, 671.
 Balick, B., Preston, H. L., and Icke, V. 1987, *A.J.*, **94**, 1641.
 Beckwith, S., Beck, S. C., and Gatley, I. 1984, *Ap. J.*, **280**, 648.
 Harpaz, A., and Kovetz, A. 1981, *Astr. Ap.*, **93**, 200.
 Kahn, F. D., and West, K. A. 1985, *M.N.R.A.S.*, **212**, 837.
 Kawabe, R., *et al.* 1987, *Ap. J.*, **314**, 322.
 Kwok, S. 1982, *Ap. J.*, **258**, 280.
 Livio, M. 1982, *Astr. Ap.*, **105**, 37.
 Livio, M., Salzman, J., and Shaviv, G. 1979, *M.N.R.A.S.*, **188**, 1.
 Livio, M., Soker, N. 1984, *M.N.R.A.S.*, **208**, 763.
 ———. 1988, *Ap. J.*, **329**, 764.
 Livio, M., Soker, N., deKool, M., and Savonije, G. J. 1986, *M.N.R.A.S.*, **218**, 593.
 Meaburn, J., Walsh, J. R., and Clayton, C. A. 1985, in *Cosmical Gas Dynamics, Proc. Manchester Conference*, ed. F. D. Kahn, p. 189.
 Mendez, R. H., Groth, H. G., Hustfeld, D., Kudritzki, R. P., and Herrero, A. 1988, *Astr. Ap.*, **197**, L25.
 Nagasawa, M., Nakamura, T., and Miyama, S. M. 1988, *Pub. Astr. Soc. Japan*, in press.
 Perek, L., and Kohoutek, L. 1967, *Catalogue of Galactic Planetary Nebulae* (Prague: Academia).
 Soker, N., and Livio, M. 1989, *Ap. J.*, in press (SL).
 Soker, N., Regev, O., Livio, M., and Shara, M. M., 1987, *Ap. J.*, **318**, 760.
 Volk, K., and Kwok, S. 1985, *Astr. Ap.*, **153**, 79.

NOAM SOKER: Department of Astronomy, University of Virginia, P.O. Box 3818, University Station, Charlottesville, VA 22903-0818